

Supporting Information

Efficient Star-Shaped Hole Transporting Materials with Diphenylethenyl Side Arms for an Efficient Perovskite Solar Cell

Hyeju Choi,^a Sojin Park,^a Sanghyun Paek,^a Piyasiri Ekanayake,^b Mohammad Khaja Nazeeruddin,^c
Jaejung Ko^{a,*}

^a Department of Advanced Material Chemistry, Korea University, 2511, Sejong-ro, Sejong City 339-700, Republic of Korea. Fax: 82-44-860-1331; Tel: 82-44-860-1337; E-mail: jko@korea.ac.kr

^b Applied Physics Program, Faculty of Science, University of Brunei Darussalam, Jalan Tungku Link, Gadong BE 1410, BRUNEI DARUSSALAM.

^c Laboratory of Photonics and Interfaces, Department of Chemistry and Chemical Engineering, Swiss Federal Institute of Technology, Station 6, CH-1015 Lausanne, Switzerland.

Contents

Figure S1. Electrochemical characterization of HTMs	2
Figure S2. Space charge limitation of current J - V characteristics of the HTMs	3
Figure S3. Histogram of the solar cell efficiencies obtained from HTMs	4
Figure S4. Photocurrent-voltage characteristics with different scan directions	5
Figure S5. Photocurrent-voltage characteristics without additives	6
Figure S6. LHE spectra of HTMs	7

Figure S1. Electrochemical characterization of the **TPA-MeOPh** and **FA-MeOPh** in dichloromethane / $(n\text{-C}_4\text{H}_9)_4\text{NPF}_6$ (0.1 M), scan speed 100 mV/s, potentials vs. Fc/Fc^+ .

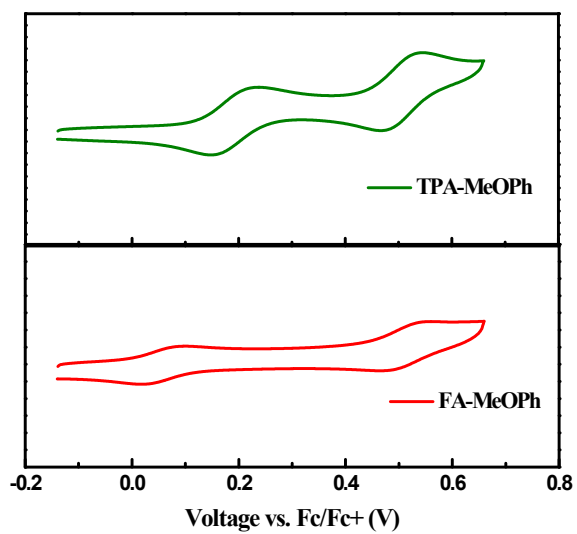
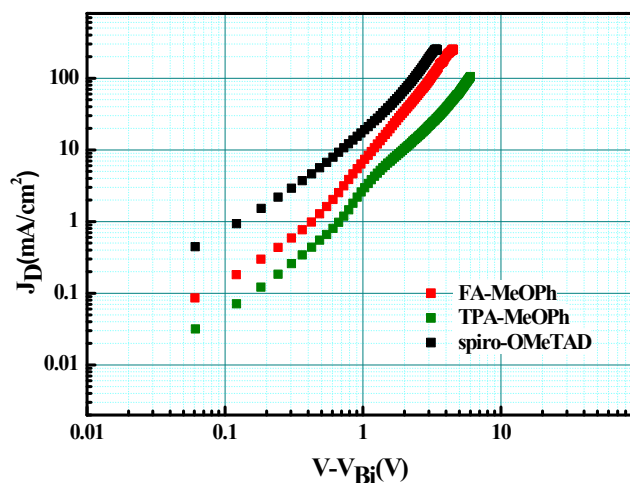


Figure S2. Space charge limitation of current J - V characteristics of the HTMs.



Space Charge Limitation of Current (SCLC). The hole mobility was investigated from the SCLC J - V characteristics obtained in the dark for hole-only devices. ITO/PEDOT:PSS/HTMs /Au devices as a function of the bias corrected by the built-in voltage determined from the difference in work function between Au and the HOMO level of HTMs. The *SCLC* behavior in the trap-free region can be characterized using the Mott-Gurney square law (1).

$$J = (9/8)\epsilon\mu(V^2/L^3) \quad (1)$$

where ϵ is the static dielectric constant of the medium and μ is carrier mobility.

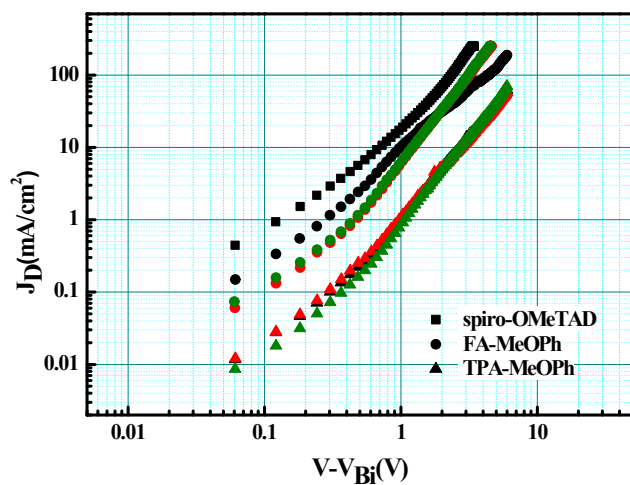
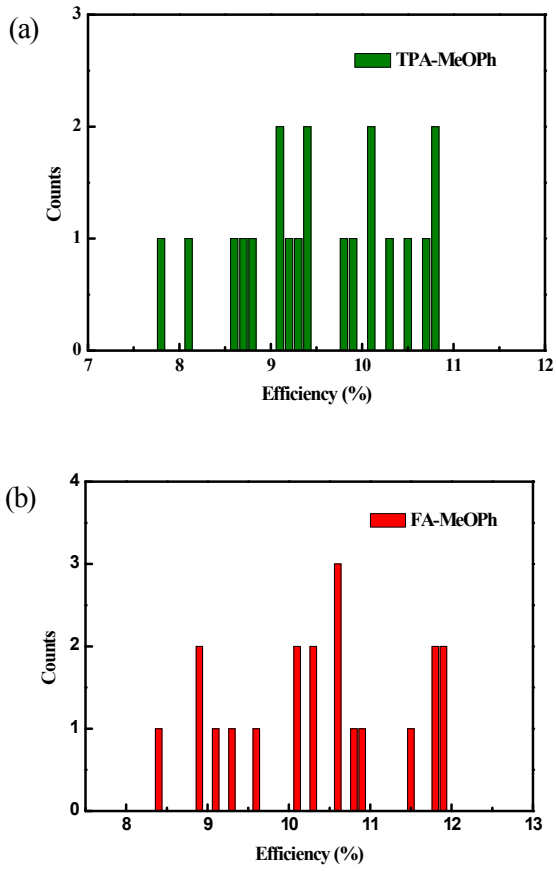
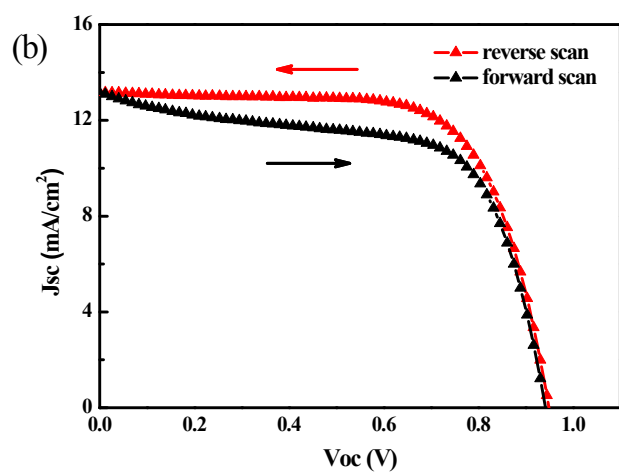
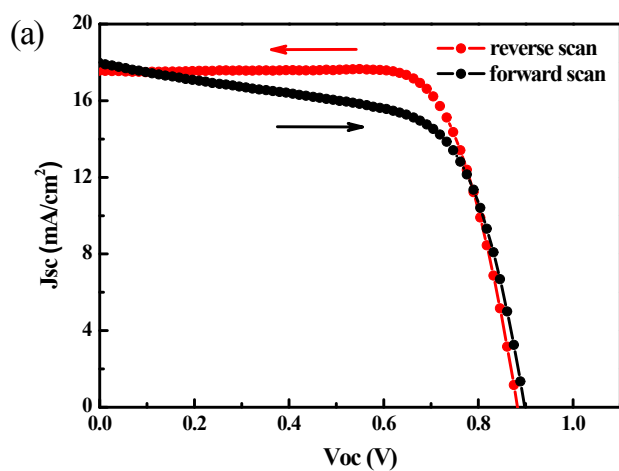


Figure S3. Histogram of the solar cell efficiencies obtained from the (a) **TPA-MeOPh** and (b) **FA-MeOPh** based hybrid solar cells.



		J_{sc} (mAcm ⁻²)	V_{oc} (V)	ff	η (%)
TPA-MeOPh	best	17.33	0.994	0.627	10.79
	average	16.16	1.001	0.616	9.94
FA-MeOPh	best	18.39	0.924	0.698	11.86
	average	17.02	0.934	0.675	10.85

Figure S4. Photocurrent-voltage (J - V) characteristics of the solar cells with (a) **FA-MeOPh** (●), (b) **TPA-MeOPh** (▲) under AM 1.5 conditions (100 mW/cm^2) with different scan directions.



		J_{sc} (mAcm^{-2})	V_{oc} (V)	ff	η (%)
FA-MeOPh	reverse	17.55	0.883	0.741	11.48
	forward	17.98	0.898	0.634	10.24
TPA-MeOPh	reverse	13.18	0.949	0.690	8.63
	forward	13.19	0.942	0.634	7.88

Figure S5. Photocurrent-voltage (J - V) characteristics of the solar cells with (a) **FA-MeOPh** (●), (b) **TPA-MeOPh** (▲) under AM 1.5 conditions (100 mW/cm²) without any additives.

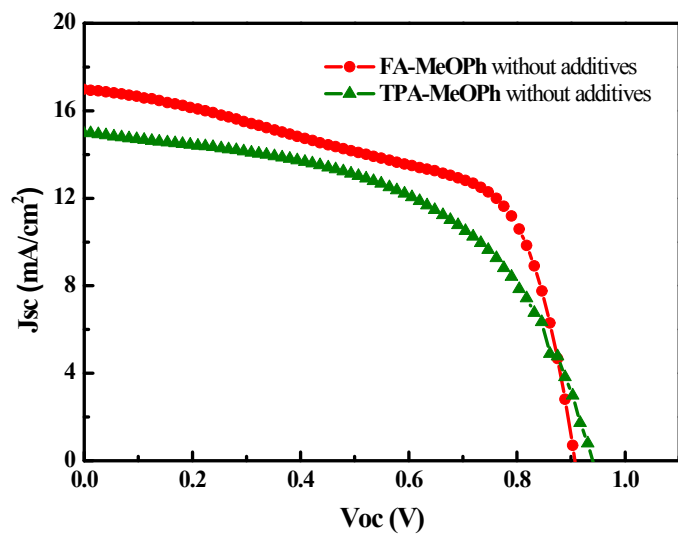


Figure S6. LHE spectra of FA-MeOPh (●) and TPA-MeOPh (▲).

